Agricultural and Forest Meteorology 213 (2015) 273–282

Contents lists available at ScienceDirect

Agricultural and Forest Meteorology

journal homepage: www.elsevier.com/locate/agrformet

Component-specific dynamics of riverine mangrove CO_2 efflux in the Florida coastal Everglades

Tiffany G. Troxler[a,*], Jordan G. Barr[b], Jose D. Fuentes[c], Victor Engel[d], Gordon Anderson[d], Christopher Sanchez[e], David Lagomasino[f], René Price[g], Stephen E. Davis[h]

[a] Southeast Environmental Research Center, OE 148, Florida International University, 11200 SW 8th Street, Miami, FL 33199, United States
[b] South Florida Natural Research Center, Everglades National Park, 40001 State Road 9336, Homestead, FL 33034, United States
[c] Pennsylvania State University, Department of Meteorology, 508 Walker Building, University Park, PA 16802, United States
[d] United States Geological Survey, Southeast Ecology Science Center, 7920 NW 71st Street, Gainesville, FL 32606, United States
[e] Abbess Center for Ecosystem Science and Policy, University of Miami, Coral Gables, FL 33146, United States
[f] Universities Space Research Association, NASA Goddard Space Flight Center, Greenbelt, MD, United States
[g] Department of Earth and Environment and Southeast Environmental Research Center, OE-148, Florida International University, Miami, FL 33199, United States
[h] Everglades Foundation, 18001 Old Cutler Road, Suite 625, Palmetto Bay, FL 33157, United States

ARTICLE INFO

Article history:
Received 2 September 2014
Received in revised form
10 December 2014
Accepted 22 December 2014
Available online 23 February 2015

Keywords:
pCO_2
Pneumatophore
Course woody debris
Carbon
Budget
Peat

ABSTRACT

Carbon cycling in mangrove forests represents a significant portion of the coastal wetland carbon (C) budget across the latitudes of the tropics and subtropics. Previous research suggests fluctuations in tidal inundation, temperature and salinity can influence forest metabolism and C cycling. Carbon dioxide (CO_2) from respiration that occurs from below the canopy is contributed from different components. In this study, we investigated variation in CO_2 flux among different below-canopy components (soil, leaf litter, course woody debris, soil including pneumatophores, prop roots, and surface water) in a riverine mangrove forest of Shark River Slough estuary, Everglades National Park (Florida, USA). The range in CO_2 flux from different components exceeded that measured among sites along the oligohaline-saline gradient. Black mangrove (*Avicennia germinans*) pneumatophores contributed the largest average CO_2 flux. Over a narrow range of estuarine salinity (25–35 practical salinity units (PSU)), increased salinity resulted in lower CO_2 flux to the atmosphere. Tidal inundation reduced soil CO_2 flux overall but increased the partial pressure of CO_2 (pCO_2) observed in the overlying surface water upon flooding. Higher pCO_2 in surface water is then subject to tidally driven export, largely as HCO_3. Integration and scaling of CO_2 flux rates to forest scale allowed for improved understanding of the relative contribution of different below-canopy components to mangrove forest ecosystem respiration (ER). Summing component CO_2 fluxes suggests a more significant contribution of below-canopy respiration to ER than previously considered. An understanding of below-canopy CO_2 component fluxes and their contributions to ER can help to elucidate how C cycling will change with discrete disturbance events (e.g., hurricanes) and long-term change, including sea-level rise, and potential impact mangrove forests. As such, key controls on below-canopy ER must be taken into consideration when developing and modeling mangrove forest C budgets.

1. Introduction

Mangrove forests cover 0.1% of the continental surface but represent an important coastal ecosystem carbon (C) pool as a result of large biomass and soil C stocks (Twilley et al., 1992; Boullion et al., 2007). For example, in a Micronesian forest, the ecosystem C stock is 400–1400 Mg C ha^{-1}, largely held within biomass and soil (Donato et al., 2011). Net annual soil C sequestration and tidal export of C are key sources of uncertainty in coastal wetland C budgets (Bauer et al., 2013), yet recently published data syntheses are beginning to reduce these uncertainties (Breithaupt et al., 2012). Carbon dioxide (CO_2) flux can occur from different components below the forest canopy including soil, fine roots, aboveground root structures (i.e., pneumatophores, prop roots), course woody debris (CWD), and when inundated, to porewater or surface water, and contribute to mangrove ecosystem respiration (ER).

* Corresponding author. Tel.: +1 305 348 1453.
E-mail address: troxlert@fiu.edu (T.G. Troxler).

http://dx.doi.org/10.1016/j.agrformet.2014.12.012
0168-1923/

Variability associated with these fluxes is reported to be a function of both physical and biological factors including temperature, duration and frequency of inundation, salinity, alkalinity, nutrient availability, root production, presence of pneumatophores, benthic microalgae, and invertebrates (Cai and Wang, 1998; Kitaya et al., 2002; Hope et al., 2004; Boullion et al., 2007; Jomura et al., 2008; Kristensen et al., 2008; Lovelock, 2008; Sasaki et al., 2009). For instance, microbial and autotrophic respiration may be limited by tidal flooding and saturation of the soil surface, whereas roots may serve as a conduit for transport of both microbial- and autotrophic-derived CO_2, in addition to microbial respiration that occurs on the decomposing wood surface. However, few datasets are available for understanding CO_2 fluxes with respect to variability induced by physical and biological factors in riverine mangrove forests.

Chamber-based CO_2 flux is a frequently used technique for determining whole-ecosystem gross primary production (GPP) and ER at the plot-scale, especially in low-stature vegetation communities (Olivas et al., 2010). In forest ecosystems, the chamber-based CO_2 flux method has been mostly used to determine CO_2 flux from the soil-atmosphere interface, whereas the eddy-flux technique is used to determine GPP and ER at the forest scale. Independently, chamber and eddy covariance techniques have limitations depending on the component and scale of interest (Thomas et al., 2008); however, coupled methods can allow for partitioning of ecosystem GPP and ER (Lavigne et al., 1997).

Our study was designed to estimate CO_2 flux rates (below-canopy respiration) as a function of both inter- and intra-site variability in a riverine mangrove system. We also sought to elucidate factors controlling below-canopy respiration fluxes that contribute to ER as a component of mangrove forest C cycling. We conducted chamber-based CO_2 flux measurements of different below-canopy components (soil, leaf litter, CWD, soil, including pneumatophores, prop roots, and surface water) over three years to quantify below-canopy CO_2 component fluxes and partition the contribution of these component fluxes to mangrove forest ER.

Key questions we sought to address were: (1) how do soil respiration rates vary along the oligohaline-saline margin? (2) What are the key components of below-canopy CO_2 flux in the near coast site? (3) How do respiration rates change seasonally and with changes in environmental controls, such as inundation, water and soil temperature? (4) How does pCO_2 vary with tidal influence in surface water and what proportion of dissolved CO_2 contributes to surface water dissolved inorganic C (DIC)? We hypothesized that: (1) soils exposed during low tide contribute to higher soil CO_2 flux than when soils are flooded with tidal water, (2) CWD contributes to the highest overall component CO_2 flux, and (3) surface water pCO_2 increases when soils are inundated.

2. Methods

2.1. Site description

The Shark River Slough (SRS) estuary discharges in the Gulf of Mexico and is located on the southwest coastal margin of the Florida Everglades within Everglades National Park (Fig. 1). The extensive riverine mangrove forests are generally dominated by red (*Rhizophora mangle*), black (*Avicennia germinans*) or white (*Laguncularia racemosa*) mangroves (Chen and Twilley, 1999). The climate of south Florida is subtropical moist (long-term annual precipitation = 155 cm yr^{-1}; average air temperature = 24 °C) with distinctive wet (June–October) and dry (November–May) seasons (Duever et al., 1994). Mangrove peat soils range from 1.5 m to 5 m in depth and are supported by a limestone platform (Wanless et al., 1994). The hydrology of the mangrove forests is driven by seasonal freshwater inputs (rainfall and overland flow) and mixed semidiurnal tides with a salinity range of 10–40 PSU. Tropical storms, winter storm fronts and freezes are key drivers of mangrove community structure and long-term ecosystem dynamics (Davis et al., 2004; Castañeda-Moya et al., 2010).

Our study sites coincide with Florida Coastal Everglades Long-Term Ecological Research (FCE LTER) program (Fig. 1). LTER sites SRS-4, SRS-5 and SRS-6 were established along a transect from the more freshwater influenced, upstream site, SRS-4, to the more saline, downstream site, SRS-6. The three sites vary most notably in vegetation structure, frequency of inundation, salinity, soil total (T) P and soil organic matter content; soil organic matter concentrations are inversely related to soil TP concentrations, and increase inland along the SRS salinity gradient (Chen and Twilley, 1999; Castañeda-Moya et al., 2013). Higher soil TP correlates with higher Ca-bound P in the lower estuary, illustrating the greater significance of mineral soil processes (Chen and Twilley, 1999) where storm-derived mineral inputs can occur (Castañeda-Moya et al., 2010). SRS-6 has been reported with greatest frequency of inundation (# tides yr^{-1}), flooding duration (h yr^{-1}) and tidal range (Castañeda-Moya et al., 2013). It is representative of tall (>15 m height) forests adjacent to the coast and Gulf of Mexico. SRS-5 is characterized by vegetation dominated by red mangrove with few black mangrove (and pneumatophores), and reported with moderate salinity, lowest frequency of inundation and moderate flood duration (Castañeda-Moya et al., 2013). SRS-4 experiences the lowest flooding duration and salinity, has the lowest TP content by volume and the highest tree density (<2.5 cm DBH; Chen and Twilley, 1999; Castañeda-Moya et al., 2013).

2.2. Tidal inundation and temperature variability

Salinity and water level data were obtained from a nearby United States Geological Survey (USGS) instantaneous recording gage (SH3) located in the riverine mangrove forest, 20 m from Shark River, and ~120 m NW of the FCE LTER site, SRS-6. Water quality data (temperature, salinity, and water level) coinciding with CO_2 flux measurements were obtained for both groundwater and surface water (gage SH3 has both a surface well [peat above limestone platform] and a groundwater well bored into the limestone bedrock to a depth of 7.3 m below the ground surface). The groundwater well water levels were measured with a pressure transducer and the surface water well water levels with a shaft-encoder float/pulley (Anderson et al., 2014). We measured soil temperature in two sites within the SRS-6 study area (January–August 2011) using Onset Hobo (Bourne, MA, USA) outdoor temperature sensors deployed just below the soil surface (~2 cm).

2.3. Carbon dioxide below-canopy efflux

We conducted extensive measurements of soil CO_2 flux (μmol CO_2 m^{-2} s^{-1}) at sites SRS-4, SRS-5 and SRS-6 of the Shark River Slough transect of the FCE LTER study area (Fig. 1). Site SRS-6 was the focus of our most intensive research. Soil CO_2 flux rates were determined with a LI-COR 8100 soil respiration system (LI-COR Biosciences, Lincoln, NE, USA) using polyvinyl chloride (PVC) collars 20 cm in diameter, inserted 2 cm into the soil. Soil collars were installed at least 1 month prior to the first set of measurements in 2008. Intact leaves not adhered to the soil surface were removed from inside the collars prior to measurements. Soil flux measurements were typically conducted at low tide. Depending on the semidiurnal tidal cycle and time of season (dry or wet), soils were exposed (no standing water on soil surface), partly exposed (partial exposure of the soil surface) or inundated (soils completely covered by surface water). In 2010, extent of standing water and

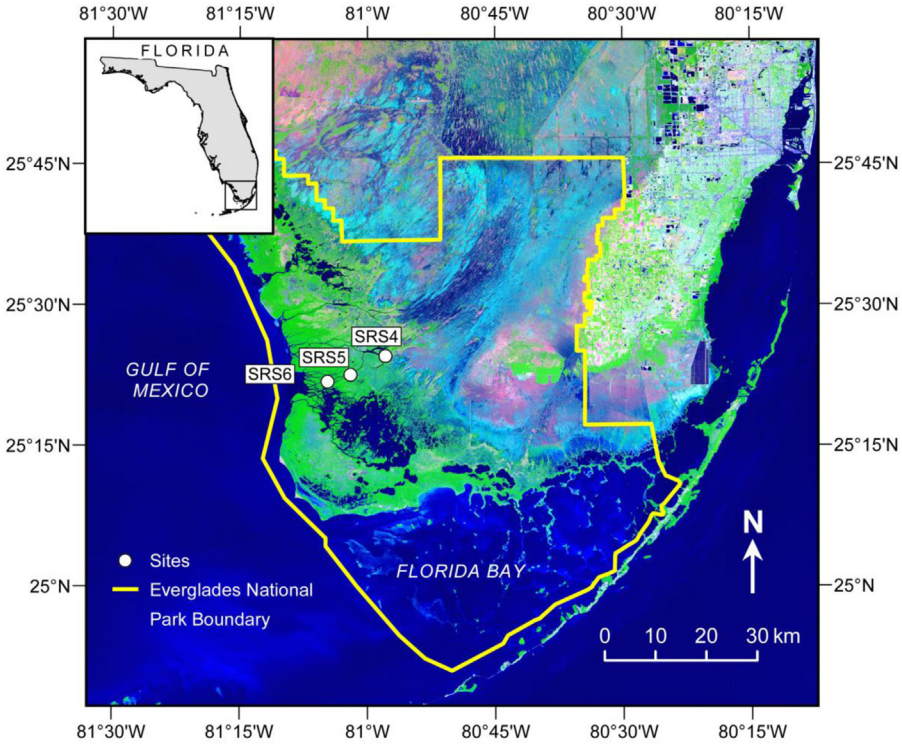

Fig. 1. Florida Coastal Everglades Long-Term Ecological Research (FCE LTER) site map including location of the 3 study sites reported in the paper: Shark River Slough (SRS) 4, 5 and 6. Map created by M. Rugge.

pneumatophore density were recorded to account for intra-site variability in soil CO_2 flux at SRS-6.

In 2011, we explicitly evaluated soil respiration fluxes as a function of black mangrove pneumatophore presence at SRS-6 by augmenting our experimental design. We installed soil collar pairs so that a pneumatophore-free soil collar had a paired collar with pneumatophores present ($N = 16$). In 2010 and 2011, measurements at SRS-6 were conducted every 1–2 months at SRS-6. Extent of standing water and pneumatophore density in each collar were recorded. The CO_2 flux from CWD was determined following the general approach of Barker (2008). Briefly, for large CWD (>20 cm diam.), collars (20 cm diam.) were cut to size and a combination of Styrofoam and silicone adhesive were used to affix the collar into a gas-tight seal on the surface of the wood. CO_2 flux from small CWD (<20 cm diam.) and red mangrove (*R.mangle*) prop roots were determined using a 10 cm PVC collar affixed to a PVC "saddle T" (Fig. 2). A gas-tight seal was created with gasket (silicone) foam and elastic nylon cords. Water–air CO_2 flux measurements were conducted by supporting the soil collar on a Styrofoam float directly over the surface of the water column, secured in place with PVC pipes to allow the height of the float to increase or decrease with change in water level. In a laboratory test, we evaluated the variation in CO_2 flux with wet mass of red mangrove leaf litter ($N = 14$). We measured CO_2 flux from wet leaf litter and converted wet weight to dry air weight.

2.4. Aqueous CO_2

In 2011, we also began measurements of in situ dissolved aqueous pCO_2. We determined concentrations of dissolved CO_2 using a non-dispersive, infrared (NDIR) sensor (Vaisala Oyj; Vanta, Finland) sealed in a water-tight, gas-permeable membrane installed 2 cm above the soil surface to be inundated by the surface water column upon tidal flooding (Tang et al., 2003; Johnson et al., 2009). We corrected sensor output for temperature and pressure using Onset Hobo water level data loggers deployed in parallel with the NDIR sensor. The NDIR sensor measurement error is 1.5% of the calibration range and 2% of the reading. We converted pCO_2 (parts per million, ppm) to concentration of dissolved CO_2 (mg L^{-1})

Fig. 2. Measurement technique for CO_2 flux from course woody debris. LI-COR 8 cm chamber affixed to a downed tree using a PVC saddle T, silicone foam and elastic cords.

following calculations determined by Weiss (1974) for CO_2 solubility as a function of temperature, pressure and salinity applying Henry's Law. Salinity, temperature, water level and atmospheric pressure data were measured and recorded using Hobo loggers. For estimation of dissolved inorganic carbon (DIC) in surface water, pH, total alkalinity, salinity, and temperature were determined on discrete water samples collected from Shark Slough at SRS-6 in May, August and November of 2011. Filtered water samples were used for total alkalinity analysis so as to remove any particulate matter, such as calcium carbonate. For total alkalinity measurements, a Brinkman Titrino 751 (Metrohm USA, Riverview, FL, USA) was used to titrate 40 mL water samples with 0.1 M hydrochloric acid to a pH of 2. The total alkalinity was calculated based on the mL of acid added at the inflection point of the titration curve closest to a pH of 4 and reported as mg L^{-1} HCO_3^-. Change in volume of the sample due to the addition of the titrant was not taken into account, as it was only a small portion of the total volume (<10%). The dissolved inorganic carbon (DIC) of the water samples was estimated as:

$$DIC = H_2CO_3^0 + HCO_3^- + CO_3^{2-} \quad (1)$$

The pCO_2 of those water samples was estimated from the total alkalinity, pH, temperature and salinity of the water samples using CO2Sys v2.1 and equilibrium constants from Millero (2010). The percent fraction of dissolved CO_2 as DIC was estimated from the average computed values of DIC in surface water.

2.5. Statistical analyses

We assessed the average difference in soil CO_2 flux rates among sites along the low-to-high salinity margin of SRS-4, SRS-5 and SRS-6. For SRS-6, we determined the variation in soil CO_2 flux with level of tidal inundation (exposed, partly exposed and inundated) using one-way ANOVA. We tested the difference in mean rates of CO_2 flux among below-canopy components of surface water, CWD, soil, prop roots, and as a function of pneumatophore presence using one-way ANOVA. We determined the controls on soil CO_2 flux using measurements when soils were exposed and no documented presence of pneumatophores at SRS-6 using stepwise regression modeling (Matlab, Mathworks, Inc., Natick, MA, USA). Candidates included the abiotic variables of water level, salinity, and water temperature data from both surface water and in a groundwater well (USGS site SH3). Predictor variables were retained in the final linear regression model for coefficients exceeding the 95% significance level ($p \leq 0.05$). Linear regression was used to develop relationships for significant factors with JMP (SAS, Cary, NC, USA).

2.6. Integration and scaling

At SRS-6, we scaled below-canopy CO_2 flux to partition ER into component fluxes and relative contribution of these fluxes to eddy-covariance based estimates of ER (Barr et al., 2010). We also generated a component-based estimate of ER based on the sum of measured components. Scaled CO_2 flux rates (kg C ha^{-1} $period^{-1}$) were determined by multiplying the fraction of surface area exposed to the atmosphere by flux rate for each component during three surface soil flooding states: when soils were exposed, partly exposed and inundated. Extent of inundation was determined from gage SH3 water level data and used to approximate the fraction of surface area of each component that was exposed to the atmosphere for each soil flooding state. Total surface area was determined from the sum of the area of all surfaces. The fraction of surface area of soil plus leaf litter was determined by the difference of the sum of course woody debris (CWD) and prop root surface area in a 1 ha area. The surface area of CWD was determined from wood volume (Krauss et al., 2005), average tree height (13 m) and diameter (10 cm). *Rhizophora* prop root surface area was determined from the relationship between average DBH (Castañeda-Moya et al., 2013), prop root biomass (Smith and Whelan, 2006), average wood density, prop root diameter of 8 cm and average prop root height of 0.5 m for *Rhizophora* (Chave et al., 2009; Zanne et al., 2009). Other methods for quantifying prop root biomass for the DBH range we estimated yielded similar values, and estimate of uncertainty at less than 2% (Feliciano et al., 2014). *Avicennia* pneumatophore surface area was derived from an estimate of pneumatophore density per tree (Dahdouh-Guebasetal et al., 2007) and *Avicenna* tree density (Castañeda-Moya et al., 2013). This estimate of pneumatophore density was within the range of that based on approximate soil oxidation-reduction potential (redox) at SRS-6 (Castañeda-Moya et al., 2013) using a relationship between soil redox and pneumatophore density developed by Thibodeau and Nickerson (1986). Leaf litter respiration was determined from an exponential relationship between leaf mass and CO_2 flux in a laboratory test ($r^2 = 0.92$, $y = -0.024x^2 + 0.531x - 0.231$, $F = 63.8$, $p < 0.0001$, $n = 14$). Leaf litter respiration was scaled to ha yr^{-1} using leaf litterfall g C m^{-2} d^{-1} (Castañeda-Moya et al., 2013). The leaf litter component accounted for floating leaves on the water surface and was added to soil respiration rates to estimate in situ soil plus leaf litter CO_2 flux. Surface area of soil plus leaf litter was 100% when soils were exposed. As such, we developed annual estimates for CO_2 (tons CO_2–C ha^{-1} yr^{-1}) flux from six components: surface water, leaf litter, soil plus leaf litter, prop roots, CWD, and soil plus pneumatophores. We binned these components into heterotrophic only (surface water, leaf litter, CWD), autotrophic only (prop roots) and heterotrophic plus autotrophic (soil plus leaf litter, soil plus pneumatophores; sum of components that could not be discretely binned) compartments of below-canopy CO_2 flux. Based on these binned components, we generated two estimates of the contribution of below-canopy components to ER where ER was determined from: (1) the sum of below-canopy respiration components, including dark leaf respiration derived from Barr et al. (2010) and (J. Barr, unpublished data), and (2) eddy-covariance (Barr et al., 2010), with the proportion of dark leaf respiration determined from the difference in ER and sum of below-canopy components measured in this study.

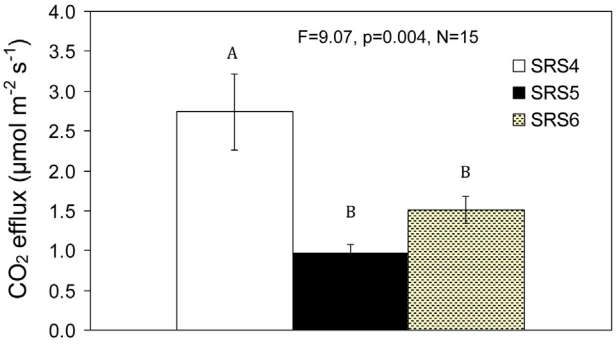

Fig. 3. Inter-site variability in soil CO_2 flux, 2008–2011. Error bars are standard error.

3. Results

3.1. Inter-site variability in soil CO_2 flux

Of the three sites, SRS-4 had the highest soil CO_2 flux rates; the difference between SRS-5 and SRS-6 was not significant (Fig. 3).

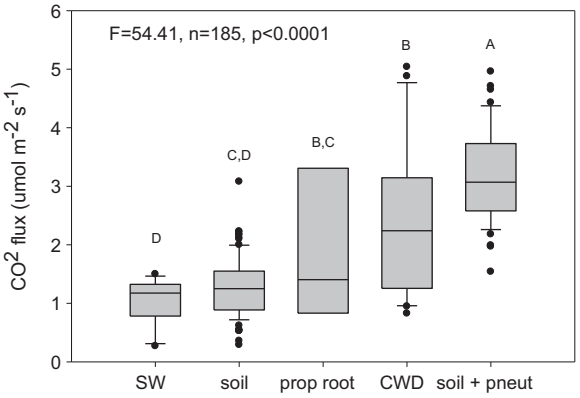

Fig. 4. Below-canopy components of CO_2 flux partitioned by surface water (SW; $n = 16$, $1.02 \pm 0.10\ \mu mol\ m^{-2}\ s^{-1}$), soil ($n = 86$, $1.27 \pm 0.05\ \mu mol\ m^{-2}\ s^{-1}$), prop roots ($n = 8$, $1.94 \pm 0.45\ \mu mol\ m^{-2}\ s^{-1}$), course woody debris (CWD; $n = 29$, $2.34 \pm 0.23\ \mu mol\ m^{-2}\ s^{-1}$), and soil with pneumatophores present (soil + pneut; $n = 47$, $3.17 \pm 0.11\ \mu mol\ m^{-2}\ s^{-1}$).

3.2. Hydrologic and temperature variability at SRS-6

Average maximum Shark River stage ranged from 0.9 m during the dry season months (December–May) to 1.01 m during the wet season months (June–November) with an average annual tidal amplitude of 1.89 m (National Park Service gage, Shark River), from years 1996–2012 (data provided by Everglades National Park). Variation in surface water inundation resulted from mixed semidiurnal tidal flooding, spring and neap tidal cycles and seasonal freshwater discharge. At SRS-6, soils were inundated, partially exposed and exposed for 81, 187, 97 days, respectively, in 2010. There was greater frequency of inundation in summer months than winter months, with surface inundation most predominant during the summer of 2010 (June–October). The greater extent of drawdown in periods between January and March 2011 coincided with a significant drought (Boucek and Rehage, 2014), as compared with 2010 during the same period.

Surface water temperature collected for the same period showed an increase of 15 °C between January and June 2010. The following year, there was a similar pattern between winter and summer surface water temperatures, with diurnal variation evident. Soil temperature, collected with sensors deployed at 2 cm soil depth, showed more dramatic decreases in overnight temperature as well as seasonal temperature. In January and February 2011, soil temperature dipped to nearly 10 °C, increasing to nearly 25 °C within days to weeks. By April 2011, the lowest soil temperature consistently exceeded 20 °C, and reached highs around 30 °C by the end of April. Soil temperatures ranged between 25 °C and 30 °C through the summer of 2011. Comparing surface water and soil temperature for the period February–May 2011 illustrates these warmer and more variable soil conditions relative to the surface water.

3.3. Intra-site variability in below-canopy CO_2 flux at SRS-6

Average CO_2 flux rates were variable among below-canopy components within SRS-6. Intra-site variability was characterized by differences between surface water, soil, prop root, CWD, and pneumatophores CO_2 fluxes (Fig. 4). For measurements conducted in 2010, CWD exhibited the highest average CO_2 flux as compared with soil and surface water. Average soil respiration, which included inundated, partially exposed, and exposed soils, was similar to CO_2 flux from surface water (Fig. 4). However, partitioning variability in soil CO_2 flux by inundation, exposed sites had higher CO_2 flux ($1.85 \pm 0.10\ \mu mol\ m^{-2}\ s^{-1}$) than those that were partially exposed ($1.27 \pm 0.19\ \mu mol\ m^{-2}\ s^{-1}$) or fully inundated ($1.29 \pm 0.18\ \mu mol\ m^{-2}\ s^{-1}$; $F = 5.56$, $p = 0.0057$). Soil respiration fluxes were consistently nearly twice as high from collars with pneumatophores present ($3.18 \pm 0.11\ \mu mol\ m^{-2}\ s^{-1}$) as compared with soil collars without pneumatophores ($1.26 \pm 0.06\ \mu mol\ m^{-2}\ s^{-1}$; $F = 240.4$, $p < 0.001$, $n = 104$; Fig. 4). When all components were considered together, CO_2 flux from soil with pneumatophores present was highest on average (Fig. 4).

Stepwise regression modeling of all abiotic parameters determined that subsurface salinity and groundwater level were the significant ($p < 0.001$) independent drivers of CO_2 flux when soils were exposed. In negative, linear relationships, soil salinity and groundwater level accounted for 0.93 and 0.70 of the variance in soil CO_2 flux, respectively (soil salinity: $y = -0.092x + 4.219$; groundwater stage: $y = -2.738x + 0.941$; Fig. 5). The decline in soil CO_2 flux occurred within the range of 26–37 PSU.

3.4. Aqueous CO_2

Surface water column concentrations of dissolved CO_2 (CO_2–C) were determined for two distinct, one-week periods of June 1–6, 2011 and August 4–9, 2011 (Fig. 6). These short-term datasets indicate CO_2–C concentrations were generally lower in June than August, but similarly increased nearly 5–10 times from baseline concentrations as the creek tide flooding inundated the soil surface. Average pCO_2 for these periods was 55 ± 2 and 194 ± 3 Pa, respectively. The range for June values was 0.38–3.19 mg CO_2–C L^{-1}, averaging 0.60 ± 0.02 CO_2–C mg L^{-1}. The range of concentrations measured in August was 1.45–5.40 mg CO_2–C L^{-1}, averaging 2.14 ± 0.04 CO_2–C mg L^{-1}. Average (±standard error) surface water temperature, salinity, pH and alkalinity used to determine DIC concentration were 27.9 ± 3.6 °C, 23.0 ± 4.3 PSU, 7.72 ± 0.18 and 264.1 ± 34.6 mg HCO_3 L^{-1}. Averaged from three measurement periods, the DIC concentration was 165 ± 80.9 mg L^{-1}. Thus, the fraction of dissolved aqueous CO_2 was approximately 1.5%.

3.5. Integration among components

Given the strong relationship between tidal inundation and ER for this mangrove forest (Barr et al., 2010), we used the extent of tidal inundation to scale the contribution of measured below-canopy fluxes over the annual cycle. We developed estimates for inundated (>0.12 m above the soil surface), partially exposed (0.03–0.12 m above the soil surface), and exposed (<0.03 m above the soil surface) soil conditions. These water levels were relative to a soil surface level that corresponded to on-site conditions where soils were inundated, partially exposed, and exposed (soil surface ~0.10–0.12 m). The extent of inundation determined the surface area of the various below-canopy components exposed to the atmosphere and, in the case of soil plus leaf litter flux, the rate of CO_2 flux applied. Overall, total below-canopy CO_2 flux was similar between periods of partially exposed soils and periods when soils were exposed (294.0 g CO_2–C m^{-2} and 304.4 g CO_2–C m^{-2}, respectively). Given the significant difference in component flux rates, this similarity in scaled annual rates was largely due to the greater duration of partially exposed soils (186 days; exposed: 97 days) in 2010. When soils were exposed, total below-canopy CO_2 flux was about 50% lower (117 g CO_2–C m^{-2}). Soil plus leaf litter CO_2 flux had the greatest contribution among components during periods when soils were exposed (152.8 g CO_2–C m^{-2}). Despite the largest CO_2 flux from soil plus pneumatophores, low pneumatophore density (i.e., *Avicennia* tree density ha^{-1}) contributed to a lower annual flux as compared with other components on

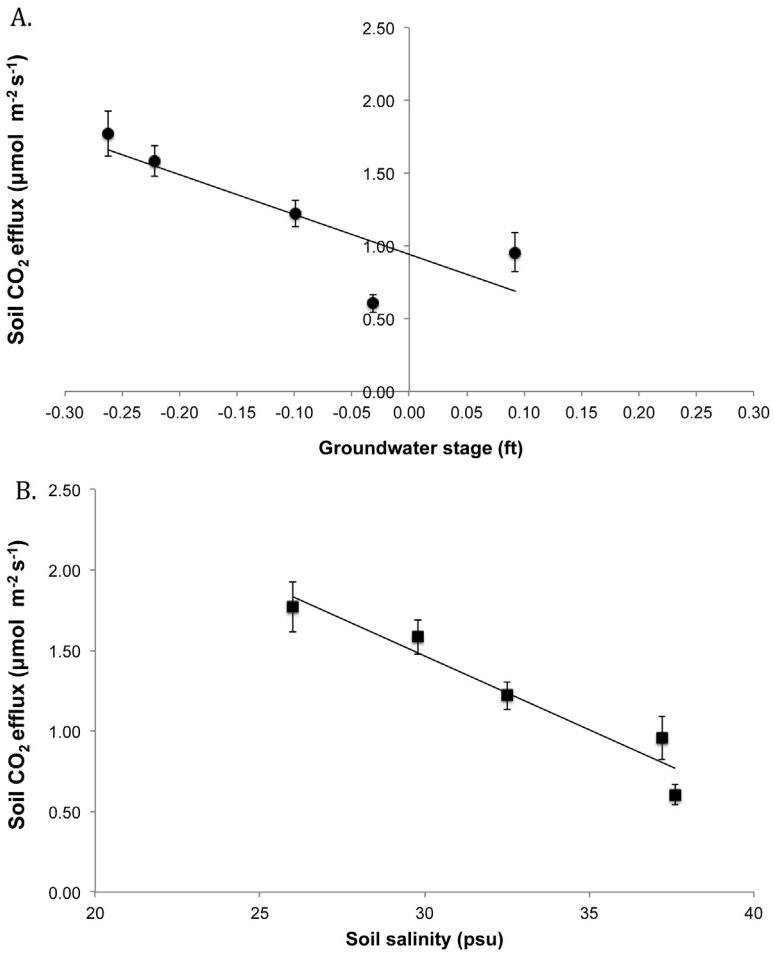

Fig. 5. Soil CO_2 efflux and (A) groundwater stage and (B) soil salinity in 2011 at SRS6. Error bars are standard error.

a ha^{-1} scale (70.5 g CO_2–C m^{-2}). We observed the contribution of CO_2 flux from surface water overlying the forest peat soil increased from 0 g CO_2–C m^{-2} when the forest peat was exposed (i.e., no surface water present) to 112.6 g CO_2–C m^{-2} when soils were partly exposed and declined to 62.8 g CO_2–C m^{-2} when soils were fully inundated.

We scaled these fluxes to CO_2–C tons ha^{-1} yr^{-1} and compared these values with measured leaf area index (J. Barr, unpublished data) and ER (Barr et al., 2010) to derive the contribution of below-canopy heterotrophic, autotrophic, heterotrophic plus autotrophic components and dark leaf respiration to mangrove forest ER. The sum of heterotrophic respiration over the three inundation periods (inundated, partially exposed and exposed) was 351.5 g CO_2–C m^{-2} yr^{-1}. The sum of autotrophic components was 140.6 g CO_2–C m^{-2} yr^{-1}. CO_2 flux of components that could not be discretely separated into heterotrophic and autotrophic respiration was 223.3 g CO_2–C m^{-2} yr^{-1}. Average dark leaf respiration at the site was 1.62 ± 1.38 mol CO_2 m^{-2} s^{-1} (Barr et al., 2010). Leaf area index (m^2 m^{-2}) averaged 2.80 ± 1.38 (J. Barr, unpublished data). Thus, dark leaf respiration was approximately 859 g CO_2–C m^{-2} yr^{-1}. The contributions of these components (below-canopy and dark leaf respiration) were derived from two different estimates of total ER: (1) ER from eddy covariance (Barr et al., 2010), and (2) the sum of all measured respiration components, including dark respiration as reported by Barr et al. (2010). We found that the sum of respiration components, including dark leaf respiration from an estimate derived from Barr et al. (2010) and J. Barr (unpublished data) exceeded that determined by eddy covariance in 2004–2005 (Table 1). Below-canopy components measured in this study contributed between 45 and 65% of total ER, depending on the estimation method for ER, i.e., sum of all components and eddy covariance with dark leaf respiration determined by difference, respectively (Table 1), suggesting below-canopy CO_2 flux contributes a greater fraction to forest ER than dark leaf respiration, regardless of estimation method used.

4. Discussion

Accumulation of soil C as peat and variability in C export associated with tidal inundation are large and highly variable components of the C budget in riverine mangrove forests (Barr et al., 2010; Adame and Lovelock, 2011; Troxler et al., 2013). Inorganic C export through CO_2 flux to the atmosphere and aqueous CO_2 loss from soil, water and pneumatophores have not been well studied. Soil CO_2 flux to the atmosphere has been shown to be comparable to terrestrial forests (Lovelock, 2008) while aqueous CO_2 export has been demonstrated to be a more significant mechanism of CO_2 loss in some mangrove forests (Maher et al., 2013). Our study documents the significant variation in direct CO_2 loss to the atmosphere associated with below-canopy soil and biogenic structures [i.e., course woody debris (CWD), prop roots, and pneumatophores] and low flux from surface water. Collectively, these fluxes comprised a significant component of the ER and suggest a larger role of below-canopy components in mangrove forest ER than previously recognized.

Table 1
The contribution of below-canopy respiration components and dark leaf respiration based on estimates of mangrove forest ecosystem respiration (ER) derived from eddy covariance and sum of all respiration components.

	Below-canopy component CO_2 efflux (tons C ha^{-1} yr^{-1})	% Contribution to ER	
		Based on eddy covariance-derived ER[a]	Based on sum of respiration components
Heterotrophic only	3.51	32	22
Autotrophic (not including dark leaf respiration) only	1.41	13	9
Heterotrophic + autotrophic	2.23	20	14
Dark leaf respiration	8.59[b]	35[c]	55
Total ecosystem respiration[d] (tons C ha^{-1} yr^{-1})	15.7		

[a] Using Barr et al. (2010) value of 11 tons C ha^{-1} yr^{-1}.
[b] Barr et al., 2010; J. Barr, unpublished.
[c] Estimated from the difference in eddy covariance value of ER (Barr et al. (2010)) and the sum of below-canopy components measured in this study.
[d] Sum of below-canopy components measured in this study and dark leaf respiration from J. Barr, unpublished.

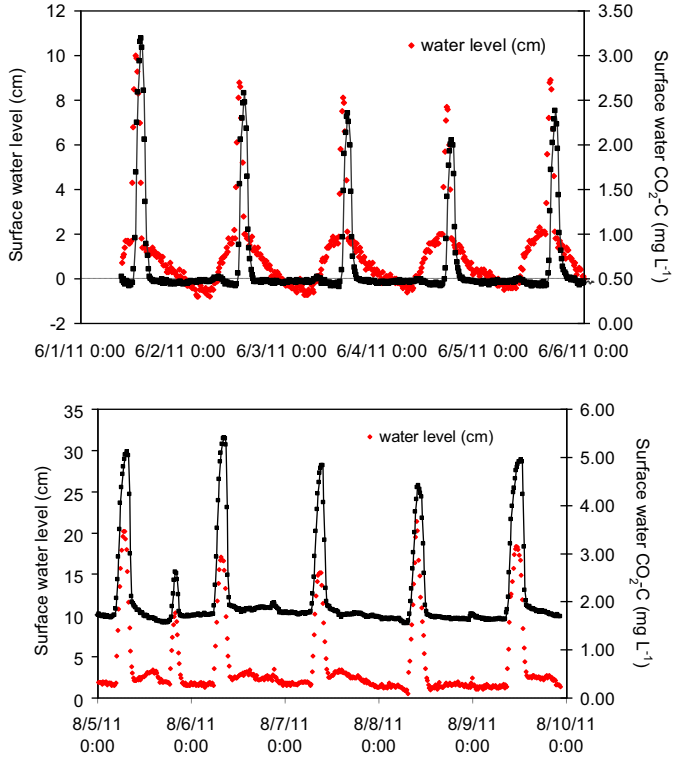

Fig. 6. Dissolved CO_2 in tidal flood water overlying the soil surface for two periods: June 1–6, 2011 and August 5–10, 2011 at SRS-6.

4.1. CO_2 flux along the coastal margin

CO_2 flux from peat soils in riverine mangroves of the Shark River Slough estuary was in the mid-upper range of soil flux rates for fringe mangroves (~0.5–2.75 μmol m^{-2} s^{-1}; Lovelock, 2008). CO_2 flux is subject to between-site variation along an oligohaline-saline coastal gradient (ecotone) with sites contrasted by vegetation structure, soil properties and frequency/duration of tidal inundation (Chen and Twilley, 1999; Castañeda-Moya et al., 2013). Longer tidal duration may have the largest influence over site differences, but salinity may also have an influence on the low soil flux rates at sites SRS-5 and SRS-6. While tidal inundation has been illustrated to be a strong driver of soil CO_2 flux in SRS-6 soils (Chambers et al., 2013), the influence of salinity in estuarine peat soils is not as well understood. A recent study conducted along a tidal freshwater–estuarine gradient in coastal marshes corresponds with our results, with higher CO_2 flux (with ecosystem respiration) from tidal freshwater marshes as compared with oligohaline and mesohaline marshes (Weston et al., 2014). Lovelock (2008) reported soil respiration from scrub and fringe forests with no significant difference between average CO_2 flux rates. Scrub forests were more consistently characterized as *Avicennia* scrub forests, which tend to occur in more saline conditions. Moreover, contributions of autotrophic and heterotrophic components need to be constrained in order to better understand the influence of salinity on microbial respiration and soil C cycling in mangrove forests.

4.2. Variation in atmospheric and aqueous CO_2 loss at SRS-6

Within the SRS-6 site, intra-site variability in CO_2 flux was complex. The range in variability among below-canopy components exceeded the variability in soil respiration among the mangrove sites sampled in this study and among fringe mangrove forests reported by Lovelock (2008). We determined several sources of variation that influenced CO_2 fluxes from below the forest canopy (i.e., soil, CWD and surface water). CO_2 fluxes varied with: (1) component measured within the below-canopy compartment, (2) pneumatophore presence, (3) level of inundation, and (4) soil salinity when soils were exposed.

Partitioning of soils with and without pneumatophores illustrated that soils with pneumatophores contributed to the highest CO_2 flux. In a mangrove forest of Okinawa, Japan, CO_2 flux from *Avicennia marina* pneumatophores (without soils) averaged 1 μmol m^{-2} s^{-1} (Kitaya et al., 2002). In our study, the difference between average values for rates of soil and soil plus pneumatophores CO_2 flux was about 1.5 μmol m^{-2} s^{-1}. In a temperate broadleaf secondary forest in Kyoto, Japan (Jomura et al., 2007), respiration from CWD was estimated as 0.50 tons C ha^{-1} yr^{-1}, about a third of our estimate (1.6 tons C ha^{-1} yr^{-1}). To our knowledge, there are no previously reported measurements of CO_2 flux from CWD in mangrove forests. Yet, hurricane disturbance events could have a significant impact on the contribution of this component to mangrove forest ER.

Comparison of CO_2 flux associated with the soil compartment and ER measured within (J. Barr, unpublished data) and above (Barr et al., 2010) the canopy shows that tidal inundation corresponds to decline in not only soil CO_2, but also CO_2 flux over the vertical forest profile and as CO_2 flux to the atmosphere. Our CO_2 flux data corroborate this mangrove ecosystem trend in two ways: (1) significantly higher below-canopy flux when soils are exposed and (2) an increase in soil CO_2 flux with decrease in groundwater stage after soils are exposed.

We found that CO_2 flux decreased with salinity within a 10 PSU range. While there were few studies that illustrated a decline in plant productivity with salinity, none reported soil CO_2 flux with variation in salinity within a site. For example, Barr et al. (2010) reported decreased photosynthetic active radiation use efficiency within a salinity range of approximately 20–35 PSU. Weston et al. (2014) reported lower maximum aboveground biomass with increased salinity in oligohaline and mesohaline marshes. Thus, as soil respiration flux captures both heterotrophic and autotrophic respiration, decreased root productivity under more saline conditions over the year may contribute to the lower rates we observed.

Flux of CO_2 from surface water (i.e., evasion; Fig. 4) was among the lowest of the below-canopy components we measured. Ho et al. (2014) measured CO_2 flux rates from open water in the Shark River in two SF6 tracer experiments as 232 ± 24 and 171 ± 20 mmol m^{-2} d^{-1}. CO_2 flux below the canopy was 50–60% lower than that measured by Ho et al. (2014), but was higher than averages reported in other studies of mangrove river CO_2 flux (40–60 mmol m^{-2} d^{-1}; Borges et al., 2003; Bouillon et al., 2008; Koné and Borges, 2008), if under continuous inundation over a 24-h period. As pCO_2 and turbulence are likely lower in surface water under the relatively closed mangrove canopy compared to the river channel, CO_2 flux in the open river could be expected to exceed the rates observed under the mangrove canopy. However, Crawford et al. (2013) found that first-order streams had higher and more variable pCO_2 and surface water CO_2 flux than higher-order streams as a result of the greater influx of shallow, CO_2-rich soil water to first-order streams. In a mangrove forest in East Timor, Alongi et al. (2012) estimated surface water CO_2 flux for six of seven sites with values ranging from 60 to 118 mmol m^{-2} d^{-1}, approximating the rates we observed.

Concentrations of dissolved CO_2 in surface water that inundated the forest soil were in the low end of the range of values determined for some peatland catchments (Billett and Moore, 2008; 2–8 mg C L^{-1}). However, few continuous measurements of dissolved CO_2 exist for tidal water overlying soil in mangrove forests. In Shark River, and in close proximity to our sites, Ho et al. (2014) reported pCO_2 in the range of 3000–4000 μatm. While tidal inundation under the mangrove canopy reduces soil CO_2 flux to the atmosphere, dissolved CO_2 concentrations in surface water were observed to increase. Although our measurement intervals were brief, trends of increased pCO_2 in surface water and low CO_2 flux from the air–water interface suggest that tidal flooding contributes to aquatic C export. This mechanism, by which carbon is respired to tidal flood waters rather than to air, has been previously identified (Romigh et al., 2006; Barr et al., 2010). In carbonate systems, these dynamics become more complex given the potential for conversion of respired CO_2 to other C forms and $CaCO_3$ precipitation or dissolution, in addition to assimilation by aquatic plants and other forms of inorganic C transformation (Liu et al., 2010; Jianhua et al., 2012).

Porewater flushing with tidal inundation followed by advective flux is suggested to be an important mechanism for C export from Shark River mangrove forests (Romigh et al., 2006). Estimates of different DIC and DOC constituents contributing to aquatic C export were estimated by Barr et al. (2010) for Shark River as 3–10 times the DOC flux, following Bouillon et al. (2008). However, direct measurements of forest-river C exchange at the scale of the mangrove ecosystem (i.e., SRS-6) for all C constituents simultaneously are still lacking.

4.3. Integration and scaling

In eddy-covariance based studies, ER is often estimated from net ecosystem exchange (NEE) and GPP, and previous results suggest that this method may underestimate ER (Thomas et al., 2008). Summing component fluxes can help to identify sources of variability, so that those components can be targeted and their contribution to ER flux partitioned (Law et al., 1999; Makiranta et al., 2008). While soil contributed a relatively small fraction of CO_2 flux in this and other previous studies (Barr et al., 2010; Lovelock, 2008), it represents only one component of the below-canopy CO_2 flux that includes soil, pneumatophores, roots and CWD.

Our study provided well-constrained values of CO_2 flux from below-canopy components in a riverine mangrove forest over a range of environmental conditions. When scaling to the forest level, estimates of surface area of the respective components and the percent of surface area that was exposed to air under three soil flooding states (exposed, partially exposed, and inundated) likely introduced uncertainties in scaled estimates. The extent to which pneumatophore density, volume of CWD and other variables described could be used to determine surface area of each below-canopy component was critical in scaling CO_2 flux to annual rates at the forest scale. For example, in a Kenyan *Avicennia* forest, Dahdouh-Guebasetal et al. (2007) showed that pneumatophore density could increase from seaward to landward positions, and with approximately 10 cm decline in surface elevation, from 200 to 2500 stems m^{-2} within a landward position. Other sources of uncertainty included components that were not included, i.e., the extent to which live mangrove branch or bole respiration contributed to ER (i.e. Clough et al., 1997) or how leaf area varies over the extent of the forest. For example, vertical surface area of trunks in the forest stand at SRS-6 may contribute to a higher proportion of below-canopy respiration, assuming that CO_2 flux from boles (tree trunks) is similar to rates from prop roots. Acknowledging these uncertainties, this analysis provided: (1) the first account of partitioned CO_2 flux for a mangrove forest and (2) an improved understanding of the relative contribution of different below-canopy components to mangrove forest ER. Integrating chamber-based component estimates as presented and discussed in this study is an effective means of constraining ecosystem-level respiration rates derived from eddy covariance methods.

This study illustrates the importance of both spatial and temporal drivers in mangrove ecosystem C balance by identifying important sources of variability in C flux that contribute to ER. Factors that drive variation in tidal inundation, salinity and vegetation structure will influence both heterotrophic and autotrophic sources and sinks of C within this riverine mangrove forest system. Shifts in the biotic and abiotic factors that influence the relative contribution of components of below-canopy CO_2 flux can help to elucidate how discrete disturbance events (e.g., hurricanes) and long-term change including sea-level rise will in turn influence carbon cycling in riverine mangrove forests.

Acknowledgements

The authors gratefully acknowledge support from the National Park Service, Florida Coastal Everglades LTER through support from the National Science Foundation grants DEB-1237517 and DBI-0620409, and the Department of Energy, National Institute for Climate Change Research (Grant number DE-FC02-06ER64298). Field support was kindly provided by Rafael Travieso, Adam Hines, Olga Sanchez and Patrick Risko. We are also grateful to two anonymous reviewers and Barclay Shoemaker who provided valuable comments that improved the manuscript. This is contribution number 704 of the Southeast Environmental Research Center at Florida International University.

References

Adame, M.F., Lovelock, C.E., 2011. Carbon and nutrient exchange of mangrove forests with the coastal ocean. Hydrobiologia 663, 23–50.

Alongi, D.M., deCarvalho, N.A., Amaral, A.L., da Costa, A., Trott, L., Tirendi, F., 2012. Uncoupled surface and below-ground soil respiration in mangroves: implications for estimates of dissolved inorganic carbon export. Biogeochemistry 109, 151–162.

Anderson, G.H., Smith, T.J., Balentine, K.M., 2014. Land-margin ecosystem hydrologic data for the coastal Everglades Florida, water years 1996–2012. U.S. Geol. Surv. Data Ser. 853, 38, http://dx.doi.org/10.3133/ds853.

Barker, J.S., 2008. Decomposition of Doulas-fir coarse woody debris in response to differing moisture content and initial heterotrophic colonization. For. Ecol. Manag. 255, 598–604.

Barr, J.G., Engel, V., Fuentes, J.D., Zieman, J.C., O'Halloran, T.L., Smith, T.J., Anderson, G., 2010. Controls on mangrove forest-atmosphere carbon dioxide exchanges in western Everglades National Park. J. Geophys. Res. 115, G02020, http://dx.doi.org/10.1029/2009JG001186.

Bauer, J.E., Cai, W.-J., Raymond, P.A., Bianchi, T.S., Hopkinson, C.S., Regnier, P.A.G., 2013. The changing carbon cycle of the coastal ocean. Nature 504, 61–70.

Billett, M.F., Moore, T.R., 2008. Supersaturation and evasion of CO_2 and CH_4 in surface waters at Mer Bleue peatland, Canada. Hydrolog. Process. 22, 2044–2054.

Borges, A.V., Djenidi, S., Lacroix, G., Théate, J., Delille, B., Frankignoulle, M., 2003. Atmospheric CO_2 flux from mangrove surrounding waters. Geophys. Res. Lett. 30 (11), 1558.

Boucek, R., Rehage, J.S., 2014. Climate extremes drive changes in functional community structure. Glob. Change Biol. 20, 1821–1831, http://dx.doi.org/10.1111/gcb.12574.

Bouillon, S., Borges, A.V., Castañeda-Moya, E., Diele, K., Dittmar, T., Duke, N.C., Kristensen, E., Lee, S.Y., Marchand, C., Middelburg, J.J., Rivera-Monroy, V.H., Twilley, R.R., Smith, T.J., 2008. Mangrove production and carbon sinks: a revision of global budget estimates. Glob. Biogeochem. Cycles 22, GB2013, http://dx.doi.org/10.1029/2007GB003052.

Boullion, S., Middleburg, J.J., Dehairs, F., Borges, A.V., Abril, G., Flindt, M.R., Ulomi, S., Kristensen, E., 2007. Importance of intertidal sediment processes and porewater exchange on the water column biogeochemistry in a pristine mangrove creek (Ras Dege, Tanzania). Biogeosciences 4, 311–322.

Breithaupt, J.L., Smoak, J.M., Smith, T.J., Sanders, C.J., Hoare, A., 2012. Organic carbon burial rates in mangrove sediments: strengthening the global budget. Glob. Biogeochem. Cycles 26 (GB3011), 11, http://dx.doi.org/10.1029/2012GB004375.

Cai, W.-J., Wang, Y., 1998. The chemistry, fluxes and sources of carbon dioxide in the estuarine waters of the Satilla and Altamaha Rivers, Georgia. Limnol. Oceanogr. 43, 657–668.

Castañeda-Moya, E., Twilley, R.R., Rivera-Monroy, V.H., 2013. Allocation of biomass and net primary productivity of mangrove forests along environmental gradients in the Florida Coastal Everglades, USA. For. Ecol. Manag. 307, 226–241.

Castañeda-Moya, E., Twilley, R.R., Rivera-Monroy, V.H., Zhang, K., Davis III, S.E., Ross, M., 2010. Sediment and nutrient deposition associated with hurricane Wilma in mangroves of the Florida Coastal Everglades. Estuar. Coasts 33, 45–58.

Chambers, L.G., Davis III, S.E., Troxler, T.G., Boyer, J.N., Downey-Wall, A., Scinto, L., 2013. Biogeochemical effects of simulated sea level rise on carbon loss in an Everglades mangrove peat soil. Hydrobiologia, http://dx.doi.org/10.1007/s10750-013-1764-6.

Chave, J., Coomes, D.A., Jansen, S., Lewis, S.L., Swenson, N.G., Zanne, A.E., 2009. Towards a worldwide wood economics spectrum. Ecology Letters 12 (4), 351–366, http://dx.doi.org/10.1111/j.1461-0248.2009.01285.x.

Chen, R., Twilley, R.R., 1999. Patterns of mangrove forest structure and soil nutrient dynamics along the Shark River Estuary, Florida. Estuaries 22, 955–970.

Clough, B.F., Ong, J.E., Gong, W.K., 1997. Estimating leaf area index and photosynthetic production in canopies of the mangrove *Rhizophora apiculata*. Mar. Ecol. Prog. Ser. 159, 285–292.

Crawford, J.T., Striegl, R.G., Wickland, K.P., Dornblaser, M.M., Stanley, E., 2013. Emissions of carbon dioxide and methane from a headwater stream network of interior Alaska. J. Geophys. Res.: Biogeosci. 118, 482–494, http://dx.doi.org/10.1002/jgrg.20034.

Dahdouh-Guebasetal, F., Kairo, J., DeBondt, R., Koedam, N., 2007. Pneumatophore height and density in relation to microtopography in the grey mangrove *Avicennia marina*. Belg. J. Bot. 140, 213–221.

Davis, S.E., Cable, J.E., Childers, D.L., Coronado-Molina, C., Day, J.W., Huttle, C.D., Madden, C.J., Reyes, E., Rudnick, D., Sklar, F., 2004. Importance of storm events in controlling ecosystem structure and function in a Florida Gulf coast estuary. J. Coast. Res. 20, 1198–1208.

Donato, D.C., Kauffman, J.B., Murdiyarso, D., Kurnianto, S., Stidham, M., Kanninen, M., 2011. Mangroves among the most carbon-rich forests in the tropics. Nat. Geosci. 4, 293–297.

Duever, M.J., Meeder, J.F., Meeder, L.C., McCollom, J.M., 1994. The climate of south Florida and its role in shaping the Everglades ecosystem. In: Davis, S.M., Ogden, J.C. (Eds.), Everglades: The Ecosystem and Its Restoration, St. Lucie, Delray Beach, FL. , pp. 225–248.

Feliciano, E.A., Wdowinski, S., Potts, M.D., 2014. Assessing mangrove above-ground biomass and structure using terrestrial laser scanning: a case study in the Everglades National Park. Wetlands, http://dx.doi.org/10.1007/s13157-014-0558-6.

Ho, D.T., Ferron, S., Engel, V.C., Larsen, L.G., Barr, J.G., 2014. Air–water gas exchange and CO_2 flux in a mangrove-dominated estuary. Geophys. Res. Lett. 41, 108–113, http://dx.doi.org/10.1002/2013GL058785.

Hope, D., Palmer, S., Billett, M.F., Dawson, J.J.C., 2004. Variations in dissolved CO_2 and CH_4 in a first-order stream and catchment: an investigation of soil–stream linkages. Hydrolog. Process. 18, 3255–3275.

Jianhua, C., Daoxian, Y., Groves, C., Fen, H., Hui, Y., Qian, L., 2012. Carbon fluxes and sinks: the consumption of atmospheric and soil CO_2 by carbonate rock dissolution. Acta Geol. Sin. 86, 963–972.

Johnson, M.S., Billett, M.F., Dinsmore, K.J., Wallin, M., Dyson, K.E., Jassal, R.S., 2009. Direct and continuous measurement of dissolved carbon dioxide in freshwater aquatic systems – method and applications. Ecohydrology 3, 68–78.

Jomura, M., Kominami, Y., Dannoura, M., Kanazawa, Y., 2008. Spatial variation in respiration from course woody debris in a temperate secondary broad-leaved forest in Japan. For. Ecol. Manag. 255, 149–155.

Jomura, M., Kominami, Y., Tamai, K., Miyama, T., Goto, Y., Dannoura, M., Kanazawa, Y., 2007. The carbon budget of coarse woody debris in a temperate broad-leaved secondary forest in Japan. Tellus 59B, 11–222.

Kitaya, Y., Yabuki, K., Kiyota, M., Tani, A., Hirano, T., Aiga, I., 2002. Gas exchange and oxygen concentration in pneumatophores and prop roots of four mangrove species. Trees 16, 155–158.

Koné, Y.J.M., Borges, A.V., 2008. Dissolved inorganic carbon dynamics in the waters surrounding forested mangroves of the Ca Mau Province (Vietnam). Estuar. Coast. Shelf Sci. 77, 409–421.

Krauss, K.W., Doyle, T.W., Twilley, R.R., Smith III, T.J., Whelan, K.R.T., Sullivan, J.K., 2005. Woody debris in the mangrove forests of south Florida. Biotropica 37, 9–15.

Kristensen, E., Bouillon, S., Dittmar, T., Marchand, C., 2008. Organic carbon dynamics in mangrove ecosystems: a review. Aquat. Bot. 89, 201–219.

Lavigne, M.B., Ryan, M.G., Anderson, D.E., Baldocchi, D.D., Crill, P.M., Fitzjarrald, D.R., Goulden, M.L., Gower, S.T., Massheder, J.M., McCaughey, J.H., Rayment, M., Striegl, R.G., 1997. Comparing nocturnal eddy covariance measurements to estimates of ecosystem respiration made by scaling chamber measurements at six coniferous boreal sites. J. Geophys. Res. 102, 977–985.

Law, B.E., Ryan, M.G., Anthoni, P.M., 1999. Seasonal and annual respiration of a ponderosa pine ecosystem. Glob. Change Biol. 5, 169–182.

Liu, Z., Dreybrodt, W., Wang, H., 2010. A new direction in effective accounting for the atmospheric CO_2 budget: considering the combined action of carbonate dissolution, the global carbon cycle and photosynthetic uptake of DIC by aquatic organisms. Earth-Sci. Rev. 99, 162–172.

Lovelock, C.E., 2008. Soil respiration and belowground carbon allocation in mangrove forests. Ecosystems 11, 342–353.

Maher, D.T., Santos, I.R., Golsby-Smith, L., Gleeson, J., Eyre, B.D., 2013. Groundwater-derived dissolved inorganic and organic carbon exports from a mangrove tidal creek: the missing mangrove carbon sink? Limnol. Oceanogr. 58, 475–488.

Makiranta, P., Minnikinen, K., Hytonen, J., Laine, J., 2008. Factors causing temporal and spatial variation in heterotrophic and rhizopheric components of soil respiration in afforested organic soil croplands in Finland. Soil Biol. Biochem. 40, 1592–1600.

Millero, F.J., 2010. Carbonate constants for estuarine waters. Mar. Freshw. Res. 61, 139–142.

Olivas, P.C., Oberbauer, S.F., Tweedie, C.E., Oechel, W.C., Kuchy, A., 2010. Responses of CO_2 flux components of Alaskan Coastal Plain tundra to shifts in water table. J. Geophys. Res. – Biogeosci., http://dx.doi.org/10.1029/2009JG001254.

Romigh, M.M., Davis III, S.E., Rivera-Monroy, V.H., Twilley, R.R., 2006. Flux of organic carbon in a riverine mangrove wetland in the Florida Coastal Everglades. Hydrobiologia 569, 505–516, http://dx.doi.org/10.1007/s10750-006-0152-x.

Sasaki, A., Hagimori, Y., Nakatsubo, T., Hoshika, A., 2009. Tidal effects on the organic carbon mineralization rate under aerobic conditions in sediments of an intertidal estuary. Ecol. Res. 24, 723–729.

Smith, T.J., Whelan, K.R.T., 2006. Development of allometric relations for three mangrove species in South Florida for use in the Greater Everglades Ecosystem restoration. Wetl. Ecol. Manag. 14, 409–419.

Tang, J., Baldocchi, D.D., Qi, Y., Xu, L., 2003. Assessing soil CO_2 efflux using continuous measurements of CO_2 profiles in soils with small solid-state sensors. Agricult. Forest Meterol. 118, 207–220.

Thibodeau, F.R., Nickerson, N.H., 1986. Differential oxidation of mangrove substrate by Avicennia germinans and Rhizophoramangle. Am. J. Bot. 73, 512–516.

Thomas, C., Martin, J.G., Goeckede, M., Siqueira, M.B., Foken, T., Law, B.E., Loescher, H.W., Katul, G., 2008. Estimating daytime subcanopy respiration from conditional sampling methods applied to multi-scalar high frequency turbulence time series. Agric. For. Meteorol. 148, 1210–1229.

Troxler, T.G., Gaiser, E., Barr, J., Fuentes, J.D., Jaffe, R., Childers, D.L., Collado-Vides, L., Rivera-Monroy, V.H., Castañeda-Moya, E., Anderson, W., Chambers, R., Chen, M., Coronado-Molina, C., Davis III, S.E., Engel, V., Fitz, C., Fourqurean, J., Frankovich, T., Kominoski, J., Madden, C., Malone, S.L., Oberbauer, S.F., Olivas, P., Richards, J., Saunders, C., Schedlbauer, J., Sklar, F.H., Smith, T., Smoak, J.M., Starr, G., Twilley, R.R., Whelan, K., 2013. Integrated carbon budget models for the Everglades terrestrial–coastal–oceanic gradient: current status and needs for inter-site comparisons. Oceanography 26, 98–107.

Twilley, R.R., Chen, R.H., Hargis, T., 1992. Carbon sinks in mangroves and their implications to carbon budget of tropical coastal systems. Water Air Soil Pollut. 64, 265–288, http://dx.doi.org/10.1007/BF00477106.

Wanless, H.H., Parkinson, R.W., Tedesco, L.P., 1994. Sea Level Control on Stability of Everglades Wetlands. In: Davis, S., Ogden, J. (Eds.), Everglades: The Ecosystem and Its Restoration. , pp. 199–224.

Weiss, R.F., 1974. Carbon dioxide in water and seawater; the solubility of a non-ideal gas. Mar. Chem. 2, 203–215.

Weston, N.B., Neubauer, S.C., Velinsky, D.J., Vile, M.A., 2014. Net ecosystem carbon exchange and the greenhouse gas balance of tidal marshes along an estuarine salinity gradient. Biogeochemistry, http://dx.doi.org/10.1007/s10533-014-9989-7.

Zanne, A.E., Lopez-Gonzalez, G., Coomes, D.A., Ilic, J., Jansen, S., Lewis, S.L., Miller, R.B., Swenson, N.G., Wiemann, M.C., Chave, J., 2009. Data from: Towards a worldwide wood economics spectrum. Dryad Digital Repository, http://dx.doi.org/10.5061/dryad.234.